Comparison of Regional Cerebral Blood Flow Responses to Hypoglycemia Using Pulsed Arterial Spin Labeling and Positron Emission Tomography

Ana Maria Arbeláez[1]*, Yi Su[2], Jewell B. Thomas[3], Amy C. Hauch[1], Tamara Hershey[2,3,4], Beau M. Ances[3]

1 Department of Pediatrics, Washington University School of Medicine, St. Louis, Missouri, United States of America, **2** Department of Radiology, Washington University School of Medicine, St. Louis, Missouri, United States of America, **3** Department of Neurology, Washington University School of Medicine, St. Louis, Missouri, United States of America, **4** Department of Psychiatry, Washington University School of Medicine, St. Louis, Missouri, United States of America

Abstract

Different brain regions sense and modulate the counterregulatory responses that can occur in response to declining plasma glucose levels. The aim of this study was to determine if changes in regional cerebral blood flow (rCBF) during hypoglycemia relative to euglycemia are similar for two imaging modalities–pulsed arterial spin labeling magnetic resonance imaging (PASL-MRI) and positron emission tomography (PET). Nine healthy non-diabetic participants underwent a hyperinsulinemic euglycemic (92 ± 3 mg/dL) – hypoglycemic (53 ± 1 mg/dL) clamp. Counterregulatory hormone levels were collected at each of these glycemic levels and rCBF measurements within the previously described network of hypoglycemia-responsive regions (thalamus, medial prefrontal cortex and globus pallidum) were obtained using PASL-MRI and [^{15}O] water PET. In response to hypoglycemia, rCBF was significantly increased in the thalamus, medial prefrontal cortex, and globus pallidum compared to euglycemia for both PASL-MRI and PET methodologies. Both imaging techniques found similar increases in rCBF in the thalamus, medial prefrontal cortex, and globus pallidum in response to hypoglycemia. These brain regions may be involved in the physiologic and symptom responses to hypoglycemia. Compared to PET, PASL-MRI may provide a less invasive, less expensive method for assessing changes in rCBF during hypoglycemia without radiation exposure.

Introduction

Hypoglycemia is a devastating problem for people with diabetes and accounts for 6–10% of all deaths of people with Type 1 diabetes [1]. Recurrent hypoglycemia in diabetes occurs due to the interplay between therapeutic hyperinsulinemia and compromised counterregulatory and symptom responses to falling plasma glucose levels. This can lead to hypoglycemia associated autonomic failure (HAAF) and can cause a vicious cycle of repeated hypoglycemia [2,3]. The exact mechanisms involved in the normal physiologic responses to hypoglycemia as well as their impairment in HAAF are not well known. A group of brain regions with glucose-sensing cells has been hypothesized to be involved [4]. These cells are unique in that they are able to translate a fall in extracellular glucose into a change in neurotransmitter or hormone release [5]. Thus, better delineation of this hypoglycemic network and how it is integrated into the hypoglycemic responses is key in order to develop novel therapeutic interventions that prevent recurrent hypoglycemia or improve hypoglycemia awareness in type 1 diabetes.

Changes in regional cerebral blood flow (rCBF) in response to hypoglycemia have been assessed using [^{15}O] water positron emission tomography (PET) [4,6,7,8]. Regional increases in rCBF may reflect increases in neuronal activity due to rises in synaptic metabolic activity but not spike firing rate [9,10,11]. Observed increases in synaptic activity in response to hypoglycemia, have been reported using PET within a discrete network of inter-connected brain regions that included the medial prefrontal cortex, orbitoprefrontal cortex, globus pallidus, thalamus, and periaqueductal grey matter [4]. These same regions are involved in modulating visceral responses [12]. In addition, increased rCBF has been observed in the dorsal midline thalamus during recurrent hypoglycemia, accompanied by attenuated counterregulatory responses due to HAAF [6]. While hypoglycemic changes in rCBF have primarily been assessed by PET, this imaging technique has significant limitations including the need for a cyclotron, significant expense, and the injection of a radiolabeled tracer thus limiting the number of studies that can be performed in a particular subject and restricting studies to adults only. More recently, non-invasive MRI methods have been developed to

assess rCBF [13] and provide comparable CBF quantification between PET and ASL; at least in euglycemia [14].

In the pulsed arterial spin labeling magnetic resonance imaging (PASL-MRI) method, arterial blood water is magnetically labeled just proximal to the region (slice) of interest. Water molecules within this portion of arterial blood are labeled magnetically. This 'paramagnetic tracer' flows into a slice of interest and exchanges with tissue water. The inflowing blood water alters tissue magnetization. During this time, the "tag" image is obtained. This process is then repeated without labeling arterial blood to create the "control" image. The difference between the "control" and "tag" image produces a perfusion image which reflects the amount of arterial blood delivered to each voxel within the slice within the transit time. PASL-MRI provides reproducible and reliable quantitative CBF measurements across the brain. Compared to PET, PASL-MRI is completely noninvasive, less expensive, has no radiation exposure risk, is performed without gadolinium, thus bypassing concerns regarding nephrogenic systemic fibrosis in patients with significant renal insufficiency and can be repeatedly performed on the same subject and on subjects of any age with great ease [15]. However, this technique has been used in only a limited number of clinical applications (i.e. brain tumors, Alzheimer's Disease or stroke) [16,17,18] and has not been widely used to study hypoglycemia or HAAF [19,20].

The aim of this study was to determine, using a within subjects study design, if PASL-MRI can detect a pattern of changes in rCBF due to hypoglycemia similar to that previously-observed with PET.

Research Design and Methods

Ethics Statement

The study was approved by the Washington University in Saint Louis (WUSTL) Human Research Protection Office. Each participant gave his or her written consent to participate in this study. All clinical investigation was conducted according to the principles expressed in the Declaration of Helsinki.

Subjects

Nine healthy adult individuals (4 women and 5 men) who were mean ±SE age 29.7±2.6 years and mean body mass index (BMI) 24.2±1.1 kg/m^2 were recruited through volunteers for health program at (WUSTL). All subjects were right handed and in good health, based on a medical history and physical examination. None were taking medications (aside from an oral contraceptive) that could affect rCBF or counterregulation. All had normal fasting plasma glucose, creatinine and hematocrit. None of the individuals had a personal or family history of diabetes in first degree relatives. None had a personal history of significant psychiatric, neurological, or cardiovascular conditions.

Experimental Design

Participants were studied in the morning after a 10-hour overnight fast. They remained supine throughout the study. Two intravenous catheters were inserted into arm veins (one for infusion of insulin and dextrose and the other for injection of radioactive isotope) and one intravenous catheter was inserted into a dorsal hand vein that was kept in a ~55°C plexiglass box (for arterialized venous sampling). All nine subjects underwent a hyperinsulinemic (regular human insulin, Novo Nordisk, Bagsværd, Denmark in a dose of 2.0 mU·kg−1·min.−1) euglycemic (92±3 mg/dL [5.1 mmol/L] ~2 hours) and then hypoglycemic (53±1 mg/dL [3.0 mmol/L]) x~2 hours) clamp procedure using variable infusions of 20% dextrose based on

plasma glucose determinations (YSI Glucose Analyzer 2, Yellow Springs Instruments, Yellow Springs, OH) every five minutes (Figure 1). During the euglycemic period, two PASL-MRI measurements of rCBF were obtained. In the second hour of euglycemia, [^{15}O]water PET measurements were performed four times at 15 minute intervals. Hypoglycemia was then induced and PET measurements were obtained four times at 15 minute intervals. Two PASL-MRI measurements were obtained at the end of the hypoglycemic clamp. Each participant was moved between the PET and MRI scanners quickly while maintaining hypoglycemic and euglycemic conditions. All scans were obtained after the subject had reached at least 20 minutes of steady state at the desired glycemic level. Every 30 minutes, arterialized venous samples were drawn for analytes (glucose, insulin, glucagon, epinephrine, norepinephrine) and blood pressures and heart rates were recorded. Throughout the study cardiac function was monitored using an electrocardiogram.

The severity of the hypoglycemic symptoms was determined every 30 minutes during the euglycemic - hypoglycemic clamp with a validated questionnaire [21]. Subjects were asked to score (from 0, none, to 6, severe) six neurogenic (autonomic) symptoms (heart pounding, shaky/tremulousness and nervous/anxious (adrenergic) and sweaty, hungry and tingling (cholinergic)) and six neuroglycopenic symptoms (difficulty thinking/confused, tired/drowsy, weak, warm, faint and dizzy) [21].

Analyte Measurements

Plasma glucose concentrations were measured with a glucose oxidase method (YSI Glucose Analyzer, Yellow Springs Instruments, Yellow Springs, OH). Plasma insulin concentrations were measured with a two site chemiluminescent assay (Immulite 1000, Siemens Corp, Los Angeles, CA). Counterregulatory hormones including plasma epinephrine and norepinephrine were measured with a single isotope derivative (radioenzymatic) method [22] and plasma glucagon concentrations were measured with a radioimmunoassay (Millipore, Temecula, CA).

Magnetic Resonance (MR) Imaging Acquisition

All MRI imaging was performed on a 1.5T Siemens Avanto System (Erlangen, Germany) with a 12 channel radiofrequency head coil. To enable computation of rCBF, a total of four proximal inversion with control for off-resonance effects (PICORE Q2) PASL-MRI perfusion scans (3 minutes in duration) were collected with two at the initiation of euglycemia and two more at the end of the hypoglycemic clamp. Scanning parameters were TR = 2500 ms, TE = 13.0 ms, TI$_1$ = 700 ms, TI$_2$ = 1800 ms, flip angle = 90°, 100 mm tag with a 10 mm gap between the tag and the imaging slice, FOV = 256 mm, 4.0×4.0×8.0 mm voxels. A total of 140 PASL-MRI frames (or 70 PASL-MRI pairs) were analyzed for each subject. One high-resolution T₁-weighted magnetization-prepared rapid gradient echo (MPRAGE) [TR = 2400.0 ms, TE = 3.23 ms TI = 1000.0 ms, flip angle = 8°, 1×1×1 mm voxels] structural scan was also obtained for anatomical region definition and facilitate image alignment.

PET Scan Acquisition

General details of the [^{15}O]water PET acquisition and analysis methods have been previously reported in detail in prior publications [6]. All PET images were acquired with a Siemens/CTI (Knoxville, TN) EXACT HR+962 tomograph using the two-dimensional mode (interslice septa extended). Subjects were positioned in the scanner so that the entire brainstem was included within the 15 cm axial field of view. A transmission scan was collected at each scan session for PET data reconstruction.
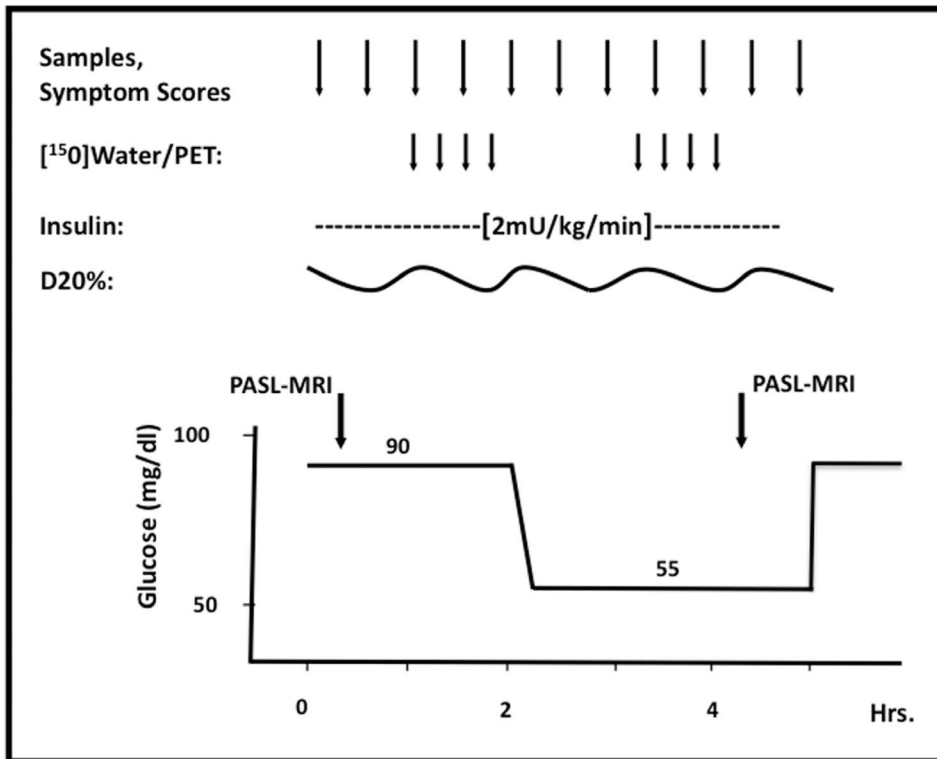
Figure 1. Schematic diagram of experimental protocol. Counterregulatory hormone levels, hypoglycemic symptom scores and rCBF measurements were obtained during the hyperinsulinemic euglycemic – hypoglycemic clamp. rCBF measurements were obtained using PASL-MRI and [15O]water PET for healthy individuals ($n = 9$).
doi:10.1371/journal.pone.0060085.g001

Four boluses of 50 mCi of [15O]water (1.85 GBq) were injected at 15 minute intervals [23,24,25] during euglycemia and repeated during hypoglycemia and 40-second emission scans were collected to measure relative rCBF.

MR Image Post-Processing

In order to evaluate the PASL-MRI data, we developed a suite of in-house image processing utilities following previously established best practices [26]. The two PASL-MRI image series for each subject were cross-aligned and motion-corrected according to a rigid body algorithm using a program developed in-house [27]. "Tag" and "control" images were pairwise subtracted to obtain mean perfusion images. CBF was calculated for each mean perfusion image using the following formula [28,29].

$$f = \frac{\lambda \Delta M}{2\alpha M_0 TI_1 \exp(-TI_2/T_{1\alpha})}$$

Where ΔM is a perfusion image calculated by pairwise subtraction of label and control images, M_0 represents the image intensity of brain tissue at magnetic equilibrium, α represents the efficiency of tag delivery, λ is blood/tissue water partition coefficient, T_{1a} is the longitudinal relaxation time of blood, and TI_1 and TI_2 are the time required to deliver the tag and the time required to collect the image, respectively. The following values were used for this study: $\alpha = 0.98$, $\lambda = 0.9$ mL/g, $T_{1a} = 1.6$ s [29].

In order to use PASL-MRI and PET methodology to assess if regional changes in rCBF occur in a-priori regions previously reported to have increased synaptic activity during hypoglycemia, each subject's MPRAGE was segmented using FreeSurfer's

segmentation and cortical reconstruction analysis software package (Freesurfer Version 5.1 developed at the Martinos Center, Harvard University, Boston, MA; http://surfer.nmr.mgh.harvard.edu) [30,31,32]. Our regional analysis primarily focused on a network of brain areas [including the thalamus (thalamus proper), medial prefrontal cortex (rostral anterior cingulate), right orbital prefrontal cortex and globus pallidum] (Figure 2) that have been shown to have increased blood flow during hypoglycemia with PET [4]. Mean rCBF of each of these regions was obtained for both glycemic conditions.

PET Scan Analyses

PET images were reconstructed using filtered back-projection technique [33]. All individual PET images were co-registered using standard technique [34] and normalized to a whole brain CBF of 50 mL/100 g/min. For each participant, the PET scans were registered to corresponding MPRAGE images using a vector-gradient based method [35]. Images from each glycemic conditions for individual subject were averaged to increase statistical precision [36]. The same regional analysis approach as the PASL-MRI data was used for PET CBF analysis.

Voxel-wise Analysis of rCBF in PET and PASL-MRI

To allow between-subject voxel-wise comparison of PET and PASL-MRI, each subject's MPRAGE data were warped to the 1988 Talairach atlas [37]. In order to eliminate anatomical differences as a possible confound in our analysis, a common atlas space was computed through an affine cross-registration of the Talairach-conformed structural scans from each individual subject [38]. For this analysis, the second PASL-MRI scan was aligned to
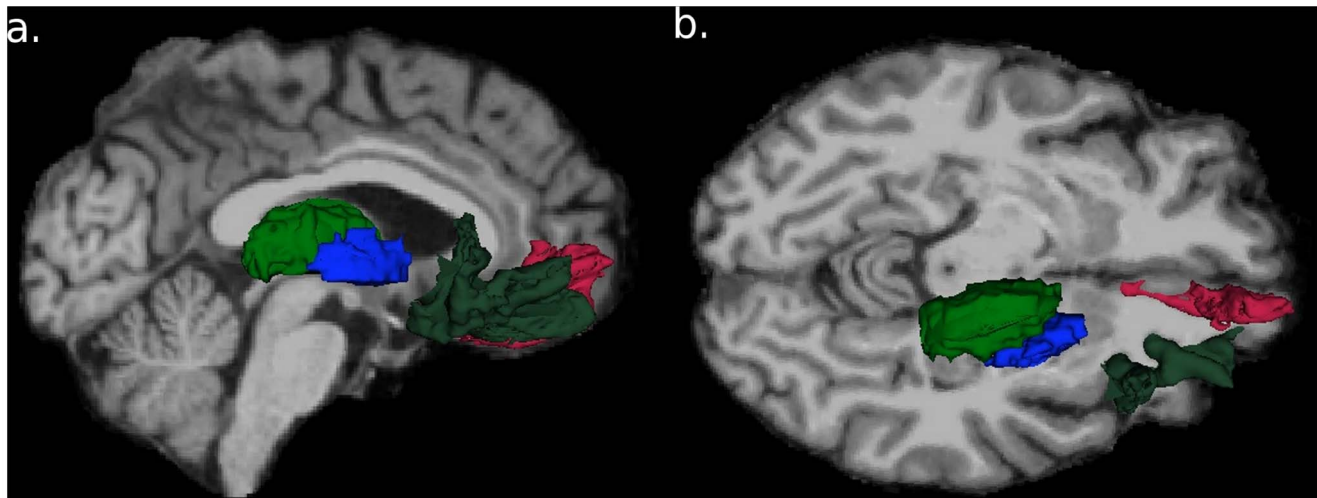
Figure 2. Free Surfer regions of interest. Free Surfer maps of ROI used for this analysis. A) Sagittal (top) B) Axial (bottom) view of Freesurfer ROIs. Blue: globus pallidum, Green: caudate, Dark Green: lateral prefrontal cortex, Magenta: medial prefrontal cortex.
doi:10.1371/journal.pone.0060085.g002

the first PASL-MRI scan. The PASL-MRI scans were aligned to a study-specific derived atlas. Each computed rCBF map (whether PET or PASL-MRI) was transformed to this study-specific atlas space after rCBF computation [26]. A voxel-wise comparison of rCBF for the two conditions (euglycemia vs. hypoglycemia) was carried out separately for PET and PASL-MRI.

Statistical Analysis

rCBF and relevant systemic variables were compared across conditions (during euglycemia vs. during hypoglycemia) using a paired t-test. P values less than 0.05 were considered significant. Hypoglycemia and euglycemia rCBF measures were expressed as means and SE. Coefficient of variation (COV) for each imaging method was calculated by computing the average SD of the rCBF from a particular region of interest (ROI) and dividing it by the mean of the rCBF from that area.

Results

Counterregulatory Hormone and Symptom Responses

During the hypoglycemic clamp plasma epinephrine responses (30±4 vs 348±37 pg/mL, p<0.0001), plasma glucagon (40±3 vs 91±3 pg/mL, p = 0.001), and cortisol (10±1 vs 21±2 μg/dL, p = 0.001) levels were significantly increased compared to euglycemia. Insulin levels during euglycemia were 160±4 vs 159±5 during hypoglycemia (p = 0.6). Hypoglycemic symptom scores significantly increased during hypoglycemia (2±0.4 vs 9±2, p = 0.005) (Table 1).

Regional Cerebral Blood Flow

During hypoglycemia, rCBF significantly increased within many ROIs for both PET and PASL-MRI (Figure 3). A significant increase in rCBF was confirmed in the thalamus (p = 0.003, p = 0.02), medial prefrontal cortex (p = 0.03, p = 0.01) and globus pallidum (p = 0.001, p = 0.01) during hypoglycemia compared to euglycemia for both PET and PASL-MRI respectively (Figure 4). The coefficient of variation across the ROI for PET was 6% and 12% for PASL-MRI, which are comparable between the two methods.

A Voxel-wise analysis of the brain using FreeSurfer's general linear model tool was utilized to assess if certain brain regions were

significantly increased for hypoglycemia for both methods. The only region that survived a multiple comparison analysis by both PASL-MRI and PET was the thalamus.

Discussion

A fall in blood glucose level below ~80 mg/dL induces a rapid counterregulatory response to restore euglycemia. This process involves the activation of peripheral and central glucose-sensing units involved in the physiological control of counterregulation. The mechanisms by which some patients with diabetes develop impaired responses to hypoglycemia remain unclear. A better understanding of these changes and the brain regions involved in the central integration of these responses, might allow targeted therapies aimed at preventing the loss of these responses in HAAF, and allow diabetic patients safer glycemic control. Our findings demonstrate that acute hypoglycemia activates the thalamus, the medial prefrontal cortex and the globus pallidum, as has previously been shown in studies using [15O]water PET [4]. These regions mediate autonomic responses to various visceral stimuli and may facilitate mechanisms due to hypoglycemia [39,40,41,42]. Although our study does not allow us to examine whether the changes seen in rCBF lead to the specific hormonal changes, based on prior studies, the thalamus has connections to the hypothalamus that can regulate the sympathoadrenal outflow during hypoglycemia, and its activation seem to be independent of awareness and be involved primarily with counterregulatory responses to hypoglycemia [7]. Meanwhile, the medial prefrontal cortex seems to be involved in counterregulation [8] and symptomatic awareness of hypoglycemia, and its activation during acute hypoglycemia may be caused by hypoglycemia per se, rather than by counterregulation [43]. Further studies are needed to outline the hierarchy of activation of brain regions and its association with hypoglycemic physiological and behavioral responses.

That we only found significant increases in rCBF in the thalamus using a voxel wise approach by both ASL and PET, does not mean that the increases in rCBF in the other regions found in the regional analysis are incorrect. A voxel-wise whole brain analysis is less sensitive in detecting changes in *a priori* identified

Table 1. Mean (±SE) plasma glucose and counterregulatory hormones at baseline and at time of CBF acquisition for euglycemic and hypoglycemic clamp phases and peak levels during each phase.

	EUGLYCEMIA			HYPOGLYCEMIA		
	Mean at Baseline	Mean during CBF acquisition	Peak value	Mean at Baseline	Mean during CBF acquisition	Peak value
Glucose (mg/dl)	91±1	92±3	101	54±1	53±1	58
Insulin	10±1	160±4	244	158±16	159±5	238
Epinephrine (pg/ml)	25±8	30±4	95	353±26	348±37	517
Glucagon (pg/ml)	59±7	40±3	62	85±11	91±3	169
Cortisol (mg/dl)	9±1	10±1	17	17±2	21±2	42
Symptoms	1±0.3	2±0.4	4	9±2	9±2	22

doi:10.1371/journal.pone.0060085.t001

regions due to correction for multiple comparisons and a factor of multiple thresholding across the entire brain space.

Although PASL-MRI has been already used in hypoglycemia studies [19,20], this study documents that PASL-MRI is a reliable method that can be used to study activation of the hypoglycemia network in a noninvasive manner since our work is the first to compare this technique to the gold standard in both conditions. PASL-MRI has several advantages, including that it is a less invasive and expensive method compared to PET, it does not require placement of an arterial line or any radiation exposure, and the scanning time can be shorter so that successive rCBF maps using PASL-MRI can be acquired on the same subject. These significant advantages encourage extension of this noninvasive imaging methodology to future pediatric studies (where less invasive methodologies are preferred) as well as to other studies of healthy and diabetic individuals, which seek to study

hypoglycemia-associated recruitment of brain regions and other hypoglycemia-associated physiological responses more broadly. Being able to study children, particularly diabetic children, offers better opportunities to understand the early loss of counter-regulatory response in recurrent hypoglycemia by allowing us to follow the full course of diabetes. However, limitations exist for PASL-MRI. It can only be performed on patients that can tolerate MRI and have no braces or metal implants that wouldn't limit the implementation of this technique. This technique also requires a very high signal-to noise ratio and cannot accurately map either low (<10 mL/100 g/minute) or high (>150 mL/100 g/minute) rCBF states [13].

The most important finding of our work is the consistent increase in rCBF due to hypoglycemia in the same regions across both imaging methods. Our work suggests that there is presence of a cerebral network involved in the hypoglycemic responses and
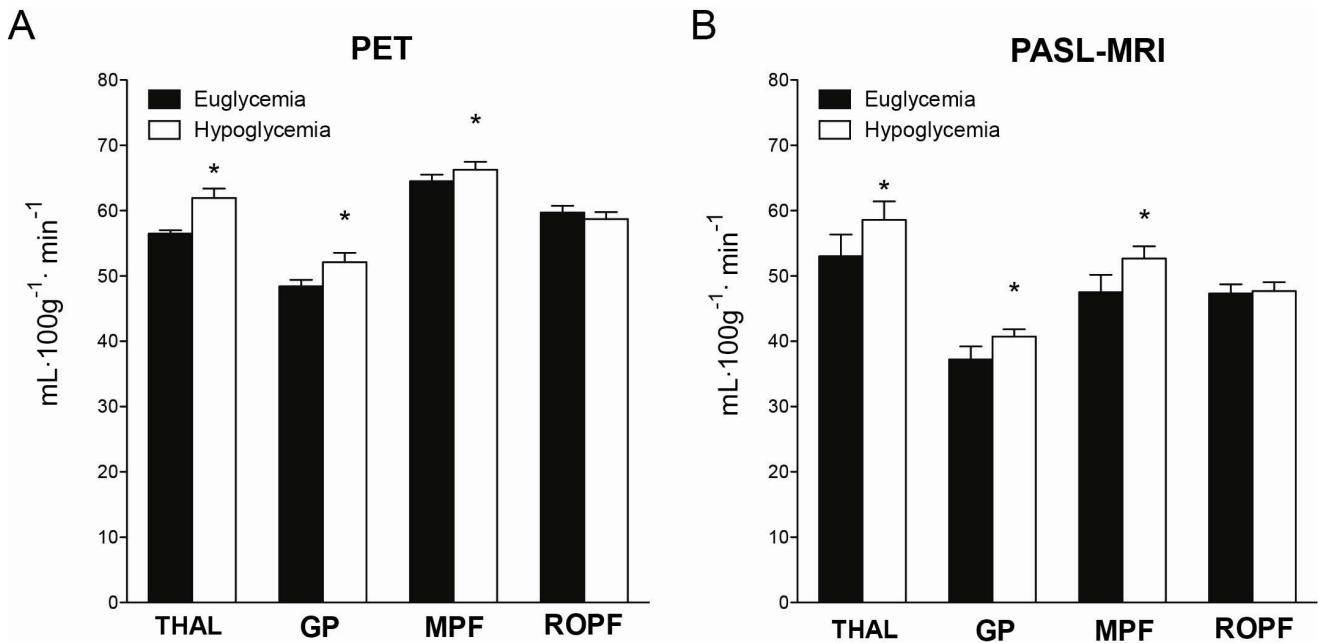

Figure 3. Qualitative cerebral blood flow during hypoglycemia and euglycemia in PET and PASL-MRI. Axial images showing the mean difference (CBF hypoglycemia – CBF euglycemia) maps from nine subjects for A) positron emission tomography (PET) and B) pulse arterial spin labeling magnetic resonance imaging (PASL-MRI). Yellow/orange represents increased and blue represents decreased blood flow during the hypoglycemic relative to euglycemic session. Similar increases in CBF for hypoglycemia were seen for both methods within the thalamus.
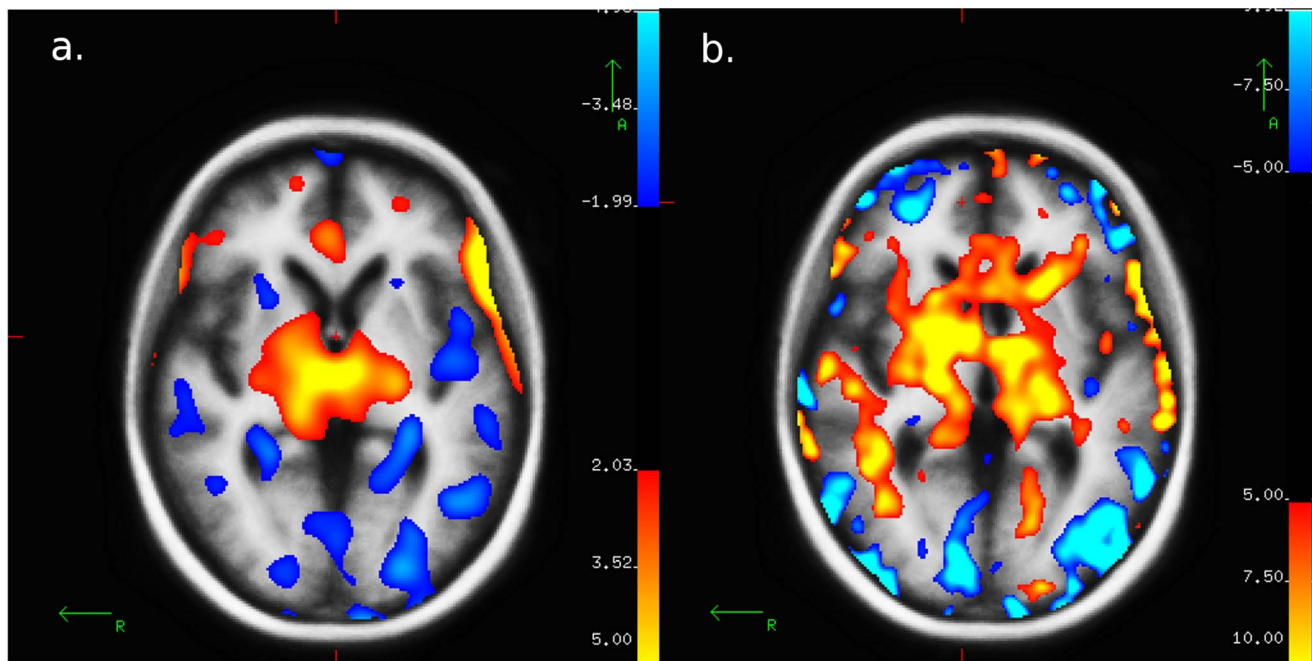doi:10.1371/journal.pone.0060085.g003

Figure 4. Quantitative regional cerebral blood flow during euglycemia and hypoglycemia in PET and PASL-MRI. Quantitative regional CBF (mL·100 g^{-1}· min^{-1}) responses for euglycemia (black bars) and hypoglycemia (white bars) within a previously identified network. Significant increases in CBF were seen with hypoglycemia within the thalamus (THAL), globus pallidum (GP), and medial prefrontal cortex (MPF) for both A) PET and B) PASL-MRI. No significant increases were seen in the right orbitoprefrontal cortex (ROPF). *p<0.05.
doi:10.1371/journal.pone.0060085.g004

demonstrates the ability to use this novel MRI method in a reliable manner to study these responses.

Acknowledgments

Author Contributions

Revised the manuscript: ACH. Conceived and designed the experiments: AMA. Performed the experiments: AMA ACH. Analyzed the data: AMA YS JBT TH BMA. Contributed reagents/materials/analysis tools: AMA YS JBT BMA. Wrote the paper: AMA YS JBT TH BMA.

References

1. Cryer PE (2008) The barrier of hypoglycemia in diabetes. Diabetes 57: 3169–3176.
2. White NH, Skor DA, Cryer PE, Levandoski LA, Bier DM, et al. (1983) Identification of type I diabetic patients at increased risk for hypoglycemia during intensive therapy. N Engl J Med 308: 485–491.
3. Bolli GB, De Feo P, De Cosmo S, Perriello G, Ventura MM, et al. (1984) A reliable and reproducible test for adequate glucose counterregulation in type I diabetes mellitus. Diabetes 33: 732–737.
4. Teves D, Videen TO, Cryer PE, Powers WJ (2004) Activation of human medial prefrontal cortex during autonomic responses to hypoglycemia. Proc Natl Acad Sci USA 101: 6217–6221.
5. McCrimmon R (2009) Glucose sensing during hypoglycemia: lessons from the lab. Diabetes Care 32: 1357–1363.
6. Arbeláez AM, Powers WJ, Videen TO, Price JL, Cryer PE (2008) Attenuation of counterregulatory responses to recurrent hypoglycemia by active thalamic inhibition: a mechanism for hypoglycemia-associated autonomic failure. Diabetes 57: 470–475.
7. Arbelaez AM, Rutlin JR, Hershey T, Powers WJ, Videen TO, et al. (2012) Thalamic activation during slightly subphysiological glycemia in humans. Diabetes Care 35: 2570–2574.
8. Teh MM, Dunn JT, Choudhary P, Samarasinghe Y, Macdonald I, et al. (2010) Evolution and resolution of human brain perfusion responses to the stress of induced hypoglycemia. Neuroimage 53: 584–592.
9. Powers WJ, Hirsch IB, Cryer PE (1996) Effect of stepped hypoglycemia on regional cerebral blood flow response to physiological brain activation. Am J Physiol 270: H554–H559.
10. Mathiesen C, Caesar K, Akgoren N, Lauritzen M (1998) Modification of activity-dependent increases of cerebral blood flow by excitatory synaptic activity and spikes in rat cerebellar cortex. J Physiol 512(Pt 2): 555–566.
11. Schwartz WJ, Smith CB, Davidsen L, Savaki H, Sokoloff L, et al. (1979) Metabolic mapping of functional activity in the hypothalamo-neurohypophysial system of the rat. Science 205: 723–725.
12. Critchley HD, Mathias CJ, Josephs O, O'Doherty J, Zanini S, et al. (2003) Human cingulate cortex and autonomic control: converging neuroimaging and clinical evidence. Brain 126: 2139–2152.
13. Wintermark M, Sesay M, Barbier E, Borbely K, Dillon WP, et al. (2005) Comparative overview of brain perfusion imaging techniques. Stroke 36: e83–e99.
14. Chen JJ, Wieckowska M, Meyer E, Pike GB (2008) Cerebral blood flow measurement using fMRI and PET: a cross-validation study. Int J Biomed Imaging 2008: 516359.
15. Detre JA, Wang J, Wang Z, Rao H (2009) Arterial spin-labeled perfusion MRI in basic and clinical neuroscience. Curr Opin Neurol 22: 348–355.
16. Deibler AR, Pollock JM, Kraft RA, Tan H, Burdette JH, et al. (2008) Arterial spin-labeling in routine clinical practice, part 2: hypoperfusion patterns. AJNR Am J Neuroradiol 29: 1235–1241.

17. Deibler AR, Pollock JM, Kraft RA, Tan H, Burdette JH, et al. (2008) Arterial spin-labeling in routine clinical practice, part 3: hyperperfusion patterns. AJNR Am J Neuroradiol 29: 1428–1435.

18. Pollock JM, Tan H, Kraft RA, Whitlow CT, Burdette JH, et al. (2009) Arterial spin-labeled MR perfusion imaging: clinical applications. Magn Reson Imaging Clin N Am 17: 315–338.

19. Page KA, Arora J, Qiu M, Relwani R, Constable RT, et al. (2009) Small decrements in systemic glucose provoke increases in hypothalamic blood flow prior to the release of counterregulatory hormones. Diabetes 58: 448–452.

20. Mangia S, Tesfaye N, De Martino F, Kumar AF, Kollasch P, et al. (2012) Hypoglycemia-induced increases in thalamic cerebral blood flow are blunted in subjects with type 1 diabetes and hypoglycemia unawareness. J Cereb Blood Flow Metab 32: 2084–2090.

21. Towler DA, Havlin CE, Craft S, Cryer P (1993) Mechanism of awareness of hypoglycemia. Perception of neurogenic (predominantly cholinergic) rather than neuroglycopenic symptoms. Diabetes 42: 1791–1798.

22. Shah SD, Clutter WE, Cryer PE (1985) External and internal standards in the single-isotope derivative (radioenzymatic) measurement of plasma norepinephrine and epinephrine. J Lab Clin Med 106: 624–629.

23. Herscovitch P, Markham J, Raichle ME (1983) Brain blood flow measured with intravenous $H_2^{15}O$. I. Theory and error analysis. J Nucl Med 24: 782–789.

24. Raichle ME, Martin WR, Herscovitch P, Mintun MA, Markham J (1983) Brain blood flow measured with intravenous $H_2^{15}O$. II. Implementation and validation. J Nucl Med 24: 790–798.

25. Videen TO, Perlmutter JS, Herscovitch P, Raichle ME (1987) Brain blood volume, flow, and oxygen utilization measured with 15O radiotracers and positron emission tomography: revised metabolic computations. J Cereb Blood Flow Metab 7: 513–516.

26. Wang Z, Aguirre GK, Rao H, Wang J, Fernandez-Seara MA, et al. (2008) Empirical optimization of ASL data analysis using an ASL data processing toolbox: ASLtbx. Magn Reson Imaging 26: 261–269.

27. Fox MD, Zhang D, Snyder AZ, Raichle ME (2009) The global signal and observed anticorrelated resting state brain networks. J Neurophysiol 101: 3270–3283.

28. Thulborn KR, Waterton JC, Matthews PM, Radda GK (1982) Oxygenation dependence of the transverse relaxation time of water protons in whole blood at high field. Biochim Biophys Acta 714: 265–270.

29. Wang J, Aguirre GK, Kimberg DY, Roc AC, Li L, et al. (2003) Arterial spin labeling perfusion fMRI with very low task frequency. Magn Reson Med 49: 796–802.

30. Desikan RS, Segonne F, Fischl B, Quinn BT, Dickerson BC, et al. (2006) An automated labeling system for subdividing the human cerebral cortex on MRI scans into gyral based regions of interest. Neuroimage 31: 968–980.

31. Fischl B, Salat DH, Busa E, Albert M, Dieterich M, et al. (2002) Whole brain segmentation: automated labeling of neuroanatomical structures in the human brain. Neuron 33: 341–355.

32. Fischl B, van der Kouwe A, Destrieux C, Halgren E, Segonne F, et al. (2004) Automatically parcellating the human cerebral cortex. Cereb Cortex 14: 11–22.

33. Cherry SR, Dahlbom M (2006) PET: Physics, Instrumentation, and Scanners; Phelps ME, editor. New York: Springer-Verlag New York Inc. 138 p.

34. Hajnal JV, Saeed N, Soar EJ, Oatridge A, Young IR, et al. (1995) A registration and interpolation procedure for subvoxel matching of serially acquired MR images. J Comput Assist Tomogr 19: 289–296.

35. Woods RP, Cherry SR, Mazziotta JC (1992) Rapid automated algorithm for aligning and reslicing PET images. J Comput Assist Tomogr 16: 620–633.

36. Ingvar M, Eriksson L, Greitz T, Stone-Elander S, Dahlbom M, et al. (1994) Methodological aspects of brain activation studies: cerebral blood flow determined with [^{15}O]butanol and positron emission tomography. J Cereb Blood Flow Metab 14: 628–638.

37. Talairach J, Tournoux P (1988) Co-planar stereotaxic atlas of the human brain: 3-dimensional proportional system: An approach to cerebral imaging. New York: Thieme Medical Publishers. 122 p.

38. Rowland DJ, Garbow JR, Laforest R, Snyder AZ (2005) Registration of [^{18}F]FDG microPET and small-animal MRI. Nucl Med Biol 32: 567–572.

39. Barbas H, Saha S, Rempel-Clower N, Ghashghaei T (2003) Serial pathways from primate prefrontal cortex to autonomic areas may influence emotional expression. BMC Neurosci 4: 25.

40. Ongur D, Price JL (2000) The organization of networks within the orbital and medial prefrontal cortex of rats, monkeys and humans. Cereb Cortex 10: 206–219.

41. Price JL (1999) Prefrontal cortical networks related to visceral function and mood. Ann NY Acad Sci 877: 383–396.

42. Raichle ME (1998) Behind the scenes of functional brain imaging: a historical and physiological perspective. Proc Natl Acad Sci USA 95: 765–772.

43. Hurst P, Garfield AS, Marrow C, Heisler LK, Evans ML (2012) Recurrent hypoglycemia is associated with loss of activation in rat brain cingulate cortex. Endocrinology 153: 1908–1914.